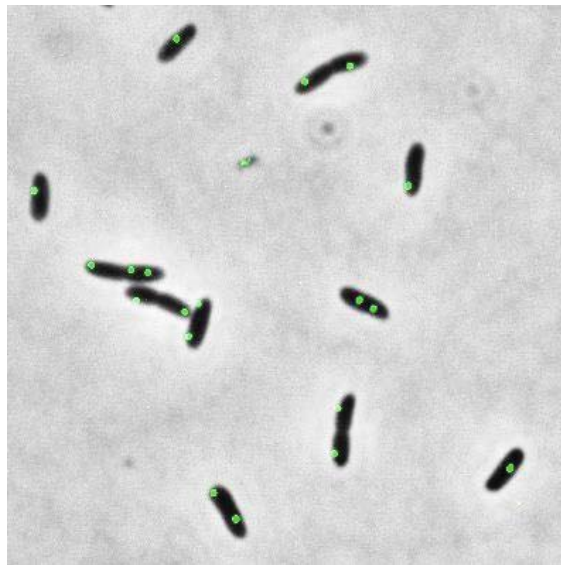


Copyright is owned by the Author of the thesis. Permission is given for a copy to be downloaded by an individual for the purpose of research and private study only. The thesis may not be reproduced elsewhere without the permission of the Author.



Massey University

DNA Replication Asynchrony in *Pseudomonas fluorescens* SBW25



A thesis presented in partial fulfillment of the requirements

for the degree of

Master of Science (Genetics)

at Massey University, Albany,

New Zealand

Akarsh Mathrani

2015

Abstract

Bacterial growth rate is largely dependent on the availability of nutrients in the environment. Past studies have shown that bacterial species such as *E. coli* can significantly increase their growth rate in nutrient-rich environments by initiating multiple cycles of DNA replication simultaneously. As a result, offspring cells not only inherit the full chromosome, but also an additional, partially replicated chromosome. However, studies have found that this multi-fork replication does not occur in all organisms such as *Caulobacter crescentus*. Detailed investigations of replication fork dynamics have thus far been limited to only a small number of bacterial species.

In this study, the cell cycle and DNA replication dynamics of *Pseudomonas fluorescens* SBW25, a gram-negative, plant-associated bacterium, is investigated. The study involves incorporating arrays of repeated operator regions bound by their fluorescently-labelled cognate repressors. A single array appears as a fluorescent focus upon live-cell imaging. An origin proximal array can therefore be visualized to follow the chromosome replication and segregation process in single living cells. Nutrient concentrations were varied in order to learn if multi-fork replication occurs in the model organism.

Results from this study show evidence for concurrent DNA replication cycles in *P. fluorescens* SBW25. This process appears to be exacerbated in nutrient-rich media (LB) as opposed to cells grown in nutrient-poor media (M9-glycerol). Moreover, asynchronous DNA replication initiations were also observed. This more stochastic initiation appears to be a common phenomenon when cells are grown in nutrient-rich media but not in nutrient-poor media. This study sheds light on a key cellular process in the *Pseudomonads*, a genus where DNA replication has not been studied extensively.

Acknowledgements

There are many individuals who have contributed and made this research possible during the course of my study. I am delighted to acknowledge their contributions.

First and foremost, I would like to thank my supervisor Dr. Heather Hendrickson for her invaluable contribution at every stage of this research. I am grateful for her continuous support, guidance and encouragement throughout this study.

I am grateful to Massey University for providing the laboratory facility for the conduct of my experiments. I am also grateful to Massey University for the financial support, which has allowed me to attend a conference during my study.

I would like to thank Dr. Brenda Youngren for providing me with various genetic tools which have made this research possible, my laboratory colleagues for their generous giving of time and support during my experimentation phase.

Finally, and most importantly, I wish to thank my parents for their continuous encouragement and support.

Table of Contents

Abstract	iii
Acknowledgements	v
Table of Contents	vi
List of Tables	viii
List of Figures	ix
Chapter 1	2
Introduction	2
1.1 Introduction	2
1.2 The Bacterial Cell Cycle	3
1.2.1 Overview.....	3
1.2.2 Growth Phase	4
1.2.3 DNA Replication.....	4
1.2.3.1 Background.....	4
1.2.3.2 DNA Replication: The Process	6
1.2.3.3 DNA Replication: Regulation	9
1.2.4 Chromosome Segregation	10
1.2.5 Cell Division	11
1.3 Multi-fork DNA Replication in Prokaryotes	12
1.4 DNA Replication and Bacterial Growth Rate	13
1.5 Previous Studies on <i>E. coli</i>	14
1.6 Multi-fork Replication Studies on Other Model Organisms	16
1.6.1 Studies on <i>V. cholerae</i>	17
1.6.2 Studies on <i>B. subtilis</i>	18
1.6.3 Studies on <i>N. gonorrhoeae</i>	20
1.6.4 Studies on <i>C. crescentus</i>	21
1.6.5 Studies on <i>P. aeruginosa</i>	22
1.7 Aims	23
1.8 Summary	24
Materials and Methods	25
2.1 Media Used for Bacterial Growth	25
2.1.1 Liquid Media: LB and M9 Glycerol 0.4%.....	25
2.1.2 Solid Media: LB Agar.....	26
2.2 Plasmid Design	26
2.2.1 Designing the ParB-GFP and parS-GMR Plasmids	26
2.2.2 Designing the pLICTRY, <i>LacO</i> -GMR and <i>TetO</i> -GMR Plasmids.....	29
2.3 Transformation Protocols	34
2.3.1 Making Chemically Competent <i>E. coli</i> DH5 α	34
2.3.2 Transformation of Chemically Competent <i>E. coli</i> DH5 α	36

2.3.3	Making Electrocompetent <i>P. fluorescens</i> SBW25	36
2.3.4	Electroporation of Electrocompetent <i>P. fluorescens</i> SBW25.....	37
2.4	Colony PCR.....	37
2.5	Agarose Gel Electrophoresis.....	40
2.6	Fluorescent Microscopy.....	40
2.6.1	Conditioning the Cells to M9 Glycerol 0.4% Media.....	40
2.6.2	Image Analysis.....	41
2.7	Growth Assays.....	42
Chapter 3	43
Integration of Non-native Fluorescently-labeled parB-parS system into <i>P. fluorescens</i>		
SBW25 Indicates Incompatibility.....		
3.1	Introduction to the ParABS System.....	43
3.2	The ParB-parS System.....	45
3.3	Results.....	46
3.4	Discussion.....	52
Chapter 4	53
Integration of LacI-lacO and TetR-tetO Systems Show Different Replication Patterns		
53		
4.1	The LacI-lacO and TetR-tetO Systems.....	53
4.2	Results.....	54
4.2.1	Building the SBW25_lacO_pLICTRY and SBW25_tetO_pLICTRY Strains	54
4.2.2	Interpretation and Analysis of Foci	61
4.3	Discussion.....	80
Chapter 5	85
Concluding Discussion		
85		
5.1	Objective of the Current Study.....	85
5.2	Summary of Results.....	86
5.2.1	Model for <i>P. fluorescens</i> SBW25 Growth in Nutrient-rich Media (from findings of both SBW25_lacO_pLICTRY and SBW25_tetO_pLICTRY strains)	86
5.2.2	Model for <i>P. fluorescens</i> SBW25 Growth in Nutrient-poor Media (from findings of SBW25_lacO_pLICTRY strain)	88
5.2.3	Model for <i>P. fluorescens</i> SBW25 Growth in Nutrient-poor Media (from findings of SBW25_tetO_pLICTRY strain)	89
5.2.4	Comparison between SBW25_tetO_pLICTRY and SBW25_lacO_pLICTRY Models in Nutrient-poor Media.....	91
5.2.4.1	Possible Explanations for SBW25_lacO_pLICTRY Cells Mostly Displaying 2 or 4 Foci	91
5.3	Future Directions	92
5.3.1	Fluorescent Microscopy	92
5.3.2	Flow Cytometry	93
Abbreviations.....		94
References		95

List of Tables

Table 1: Summary of all the strains with their genetic features in relation with the ParB- <i>parS</i> system.....	47
Table 2: Quantification of FeCl ₃ induced fluorescent background noise reduction in WT SBW25 and SBW25_ <i>parS</i> _ParB-GFP cells.....	50
Table 3: Summary of all the strains with their genetic features in relation with the LacI- <i>lacO</i> and TetR- <i>tetO</i> systems.....	55
Table 4: Doubling time of WT SBW25, SBW25_ <i>lacO</i> _pLICTRY and SBW25_ <i>tetO</i> _pLICTRY strains in LB and M9 0.4% Glycerol media, during exponential growth. The doubling times were calculated from the growth curves between 0.4 and 0.6 OD ₆₀₀ from Figure 22.....	59
Table 5: Table showing the proportions of SBW25_ <i>lacO</i> _pLICTRY and SBW25_ <i>tetO</i> _pLICTRY populations that undergo asynchronous DNA replication initiation when grown in LB or M9 0.4% Glycerol media. .	68
Table 6: List of Abbreviations.....	94

List of Figures

Figure 1: Diagrams showing standard eukaryotic and prokaryotic cell cycles during continuous growth. The length of arrows represent the duration of the phase being carried out. * Multi-fork DNA replication is explained in section 1.3.....	3
Figure 2: Diagram showing the theta replication model for DNA replication in bacteria (adapted from John Cairns, 1961 [11]).	5
Figure 3: A schematic diagram illustrating the recruitment of replisomes onto <i>oriC</i> locus by DnaA.	7
Figure 4: Diagram showing a replication fork and its components.	8
Figure 5: Diagram showing the multi-fork replication model for DNA replication in prokaryotic organisms (adapted from Skarstad, <i>et al.</i> , 1986 [48]).	13
Figure 6: Illustration of chromosomal organization inside an <i>E. coli</i> cell at various stages of its cell cycle during slow and fast growth (source: Wang & Rudner, 2014 [62]).	16
Figure 7: Diagram showing the cell cycle of <i>V. cholerae</i> (source: Rasmussen, <i>et al.</i> 2007 [70]).	18
Figure 8: Illustration of chromosomal organization inside a <i>B. subtilis</i> cell during various stages of its cell cycle (source: Wang & Rudner, 2014 [62]).	19
Figure 9: Diagram showing the current understanding of the <i>C. crescentus</i> cell cycle (source: Skerker & Laub, 2004 [65]).	21
Figure 10: An Illustration of the chromosomal organization inside a <i>P. aeruginosa</i> PAO1 cell during various stages of its cell cycle (source: Wang & Rudner, 2014 [62]).	23
Figure 11: Plasmid map of the ParB-GFP plasmid.	27
Figure 12: Plasmid map of the <i>parS</i> -GMR plasmid.	29
Figure 13: Plasmid map of the pLICTRY plasmid.	30
Figure 14: Plasmid map of the <i>lacO</i> -GMR plasmid.	31
Figure 15: Plasmid map of the <i>tetO</i> -GMR plasmid.	33
Figure 16: Picture of a gel depicting the results from a typical colony PCR reaction.	38
Figure 17: An illustration of the genetic organization of a <i>par</i> operon (Adapted from Gerdes, Howard & Szardenings 2010 [98]).	44
Figure 18: (A) Measuring GFP expression of SBW25 <i>parS</i> -GFP cells without IPTG induction using flow cytometry and fluorescent microscopy. (B) Measuring GFP expression of SBW25 <i>parS</i> _ParB-GFP cells with IPTG induction using flow cytometry and fluorescent microscopy. (C) <i>P. fluorescens</i> SBW25 with suitable foci.	48
Figure 19: Image depicting which regions of the SBW25 <i>parS</i> _ParB-GFP cells were considered to be ‘background noise’ and ‘foci fluorescence’. Red arrows point to locations considered as ‘‘foci fluorescence’’ and yellow arrows point to locations considered as ‘‘background noise’’.....	49
Figure 20: (A) Foci comparison between SBW25 <i>parS</i> _ParB-GFP cells grown in nutrient-rich media (LB) and SBW25 <i>parS</i> _ParB-GFP cells grown in nutrient-poor media (M9 0.4% glycerol). The images have been treated with ‘Hatrick Filter’, a plugin for ImageJ, the image analysis software used. Hatrick Filter is used to decrease background noise. (B) Foci comparison between SBW25 <i>parS</i> _ParB-GFP cells and SBW25 ParB-GFP cells. Both of the samples were grown in nutrient-poor media (M9 0.4% glycerol)...	51
Figure 21: Typical field of view of SBW25 <i>lacO</i> _pLICTRY cells and SBW25 <i>tetO</i> _pLICTRY cells when grown in both LB media and M9 0.4% Glycerol media. The raw images have been treated with ‘Hatrick Filter’, a plugin for ImageJ, the image analysis software used. Hatrick Filter is used to decrease background noise.	56
Figure 22: Growth Assay of WT SBW25, SBW25 <i>lacO</i> _pLICTRY and SBW25 <i>tetO</i> _pLICTRY strains in LB and M9 0.4% Glycerol media, with and without the presence of antibiotics. All the values presented are the averages of sample triplicates. The error bars denote standard error. (A) Growth curves of all the strains in nutrient-rich media (LB). (B) Growth curves of all the strains in nutrient-poor-media (M9 0.4% Glycerol). The fluctuating growth of the SBW25 <i>lacO</i> _pLICTRY strains in M9 0.4% Glycerol media indicates unstable growth.	58
Figure 23: Charts showing the average CFU counts of SBW25 <i>lacO</i> _pLICTRY cells when plated on LB only and various LB + antibiotic plates, following overnight incubation in a liquid LB culture with and without the presence of antibiotic selection pressures. The error bars denote standard error. (A) Average CFU counts of cells plated on various plates following overnight incubation in liquid LB culture without the presence of antibiotic selection pressures. (B) Average CFU counts of cells plated on various plates following overnight incubation in liquid LB culture with the presence of antibiotic selection pressures. ...	60
Figure 24: Charts showing results of fluorescent microscopy analysis of both SBW25 <i>lacO</i> _pLICTRY and SBW25 <i>tetO</i> _pLICTRY strains grown in LB and M9 0.4% Glycerol media. The error bars denote	

standard error. (A) Shows the proportions of cells containing varying numbers of foci, in the SBW25_ *lacO*_pLICTRY population grown in LB media. (B). Shows the average cell lengths within the sub-populations presented in A. (C). Shows the proportions of cells containing varying numbers of foci, in the SBW25_ *tetO*_pLICTRY population grown in LB media. (D). Shows the average cell lengths within the sub-populations presented in C. (E). Shows the proportions of cells containing varying numbers of foci, in the SBW25_ *lacO*_pLICTRY population grown in M9 0.4% Glycerol media. (F). Shows the average cell lengths within the sub-populations presented in E. (G). Shows the proportions of cells containing varying numbers of foci, in the SBW25_ *lacO*_pLICTRY population grown in M9 0.4% Glycerol media. (H). Shows the average cell lengths within the sub-populations presented in G. 64

Figure 25: Image showing SBW25_ *lacO*_pLICTRY cells when viewed under the fluorescent microscope after growth in nutrient-poor media until stationary phase was reached (OD = ~ 1.5). Cells displaying a yellow outline are likely a product of the interaction between Hatrick Filter and cells overexpressing the fluorescent proteins. 67

Figure 26: Plots showing lengths and foci locations within those lengths, of individual cells in exponential growth, from populations of SBW25_ *lacO*_pLICTRY and SBW25_ *tetO*_pLICTRY strains grown in LB & M9 0.4% Glycerol media. A. Shows data from SBW25_ *lacO*_pLICTRY cells when grown in LB. B. Shows data from SBW25_ *lacO*_pLICTRY cells when grown in M9 0.4% Glycerol. C. Shows data from SBW25_ *tetO*_pLICTRY cells when grown in LB. The dotted red circle represents a group of foci which may have been counted as ‘first focus’, although they could potentially be ‘second focus’ instead. If this is true, then the cells containing those foci will be 4 foci cells instead of 3 foci cells as categorized. D. Shows data from SBW25_ *tetO*_pLICTRY cells when grown in M9 0.4% Glycerol. (Note: It is worth noting that when measuring the cell pole to foci distance, the focus that was more distant from the pole was always considered to be the first focus). 73

Figure 27: Charts showing the overlap between cell length ranges of cell populations from SBW25_ *lacO*_pLICTRY and SBW25_ *tetO*_pLICTRY strains consisting varying numbers of foci, when grown in nutrient-rich (A) and nutrient-poor (B) conditions. 74

Figure 28: The above plots present the same data as from Figure 26, however instead of showing foci localizations inside individual cells, here we can see individual foci distributions of the whole population of SBW25_ *lacO*_pLICTRY and SBW25_ *tetO*_pLICTRY strains when grown to exponential phase in LB and M9 0.4% Glycerol media. The populations are divided into groups based on cell ages (*i.e.* cell lengths) and number of foci within the cells. (A). Shows data from the population of SBW25_ *lacO*_pLICTRY cells when grown in LB media. (B). Shows data from the population of SBW25_ *lacO*_pLICTRY cells when grown in M9 0.4% Glycerol media. (C). Shows data from the population of SBW25_ *tetO*_pLICTRY cells when grown in LB media. (D). Shows data from the population of SBW25_ *tetO*_pLICTRY cells when grown in M9 0.4% Glycerol media. 79

Figure 29: A schematic representation of the model hypothesized for the growth of *P. fluorescens* SBW25 in nutrient-rich conditions (from the findings of both SBW25_ *lacO*_pLICTRY and SBW25_ *tetO*_pLICTRY strains). 87

Figure 30: A schematic representation of the model hypothesized for the growth of *P. fluorescens* SBW25 in nutrient-poor conditions (from the findings of SBW25_ *lacO*_pLICTRY strain). 89

Figure 31: A schematic representation of the model hypothesized for the growth of *P. fluorescens* SBW25 in nutrient-poor conditions (from the findings of SBW25_ *tetO*_pLICTRY strain). 90

